Journal of Neuroscience Methods 219 (2013) 233–239

Contents lists available at ScienceDirect

Journal of Neuroscience Methods

journal homepage: www.elsevier.com/locate/jneumeth

Computational Neuroscience

Investigating the interaction between heart rate variability and sleep EEG using nonlinear algorithms

Jia-Rong Yeh[a], Chung-Kang Peng[a,b], Men-Tzung Lo[a,**], Chien-Hung Yeh[a], Shih-Ching Chen[c], Cheng-Yen Wang[a], Po-Lei Lee[d], Jiunn-Horng Kang[c,e,*]

[a] Research Center for Adaptive Data Analysis and Center for Dynamical Biomarkers and Translational Medicine, National Central University, Taoyuan, Taiwan
[b] Rey Institute for Nonlinear Dynamics in Medicine, Harvard Medical School, Boston, MA, USA
[c] Department of Physical Medicine and Rehabilitation, School of Medicine, College of Medicine, Taipei Medical University, Taipei, Taiwan
[d] Department of Electrical Engineering, National Central University, Taoyuan, Taiwan
[e] Sleep Center, Taipei Medical University Hospital, Taipei, Taiwan

HIGHLIGHTS

- A new model for monitoring the sleep stages is built based on Hilbert Huang transform.
- Two main oscillations were defined to depict the feature of sleep EEG based on HHT.
- Slow- and fast-waves oscillations correspond to fluctuations in the delta and high frequency band.
- DFA $\alpha 1$ was used to reflect the ANS activity during sleep.
- The relationship between sleep EEG and HRV was significantly confirmed in this study.

ARTICLE INFO

Article history:
Received 4 July 2013
Received in revised form 2 August 2013
Accepted 5 August 2013

Keywords:
Sleep EEG
Sympathovagal modulation
Heart rate variability
Hilbert Huang transform
Detrended fluctuation analysis

ABSTRACT

Background: The multi-mode modulation is a key feature of sleep EEG. And the short-term fractal property reflects the sympathovagal modulation of heart rate variability (HRV). The properties of EEG and HRV strongly correlated with sleep status and are interesting in clinic diagnosis.
New method: 19 healthy female subjects were included for over-night standard polysomnographic study. Hilbert Huang transform (HHT) was used to characterize the temporal features of slow- and fast-wave oscillations decomposed from sleep EEG at different stages. Masking signals were used for solving the mode-mixing problem in HHT. On the other hand, detrended fluctuation analysis (DFA) was used to assess short-term property of HRV denoted as DFA $\alpha 1$, which reflects the temporal activity of autonomic nerve system (ANS). Thus, the dynamic interaction between sleep EEG and HRV can be examined through the relationship between the features of sleep EEG and DFA $\alpha 1$ of HRV.
Results: The frequency feature of sleep EEG serves as a good indicator for the depth of sleep during non-rapid eye movement (NREM) sleep, and amplitude feature of fast-wave oscillation is a good index for distinguishing rapid eye movement (REM) from NREM sleep.
Comparison with existing method: The relationship between DFA $\alpha 1$ of HRV and the mean amplitude of fast-wave oscillation of sleep EEG affirmed with Pearson correlation coefficient is more significant than the correlation verified by the traditional spectral analysis.
Conclusion: The dynamic properties of sleep EEG and HRV derived by EMD and DFA represent important features for cortex and ANS activities during sleep.

1. Introduction

Clinical studies have shown that acute stress affects heart rate variability during sleep (Hall et al., 2004), particularly slow-wave sleep, which is thought to be associated with a "restorative" or "refreshing" sensation (Tasali et al., 2008). The dynamic interactions between EEGs and cardiac autonomic function during sleep have only been explored and reported using fast Fourier transform

* Corresponding author at: Sleep Center, Taipei Medical University Hospital, 252 Wu Hsing Street, Taipei 110, Taiwan. Tel.: +886 2 27372181x1236.
** Corresponding author at: Research Center for Adaptive Data Analysis, National Central University, Chungli, Taiwan, Tel: +886 3 4227151x34952.
E-mail addresses: mzlo@ncu.edu.tw (M.-T. Lo), jhk@tmu.edu.tw (J.-H. Kang).

0165-0270/$ – see front matter © 2013 Elsevier B.V. All rights reserved.
http://dx.doi.org/10.1016/j.jneumeth.2013.08.008

based (FFT-based) analysis (Jurysta et al., 2003). Those properties of sleep electroencephalogram (EEG) and heart rate variability (HRV) have been used in many clinical diagnoses, such as sleep apnea syndrome (Roche et al., 1999; Jurysta et al., 2006), depressive disorder (Jurysta et al., 2010), and acute schizophrenia (Boettger et al., 2006).

In traditional sleep medicine, human sleep is polygraphically defined by stages 1, 2, 3, 4 of non-rapid eye movement (NREM) sleep and rapid eye movement (REM) sleep, according to the "Manual of Standardized Terminology, Techniques and Scoring System for Sleep Stages of Human Sleep" proposed by Rechtschaffen and Kales (R-K criteria) (Rechtschaffen and Kales, 1968). The four stages of NREM sleep are denoted as NREM1, NREM2, NREM3, and NREM4. Spectral analysis uncovers more detailed sleep fluctuations beneath the continuous fluctuating pattern of EEG signals during sleep (Uchida et al., 1992, 1994, 1999). On the other hand, the dynamics of HRV serves as a good assessment of autonomic nerve system (ANS) activity during sleep (Mina et al., 2003). Spectral analysis is commonly used in the investigations associated with sleep EEG and HRV (Mina et al., 2003; Otzenberger et al., 1997, 1998; Ehrhart et al., 2000; Brandenberger et al., 2001).

However, both sleep EEG and HRV are nonlinear and non-stationary signals. In this study, we aimed to re-investigate the features of sleep EEG and the dynamic properties of HRV based on two innovative analysis algorithms, which were particularly developed for analyzing nonlinear and non-stationary signals. Empirical mode decomposition (EMD) is the first nonlinear algorithm for decomposing a time series into a finite number of intrinsic mode functions (IMFs) (Huang et al., 1998). In addition, the frequency and amplitude modulations of an IMF can be derived by Hilbert transform. The association of EMD and Hilbert transform is named as Hilbert Huang transform (HHT). The second algorithm is detrended fluctuation analysis (DFA) (Peng et al., 1995a), which serves to quantify the fractal property of signals. The short-term (scales 4–11) fractal property of human heart beat time series denoted as DFA α_1 represents a state function of autonomic nerve system (ANS) during sleep (Tulppo et al., 2005; Penzel et al., 2003). A high value of DFA α_1 represents an active state of ANS, often observed during REM sleep. A low value of DFA α_1 represents an inactive state of ANS, often observed during slow wave sleep (SWS).

In this study, sleep EEG recordings were decomposed into a set of IMFs by EMD. Two major oscillations denoted as slow-wave (SW) and fast-wave (FW) oscillations were reconstructed using IMFs according to the averaged frequencies of IMFs. Both SW and FW oscillations were smoothed by moving average to represent two major oscillatory fluctuations of sleep EEG. Furthermore, Hilbert transform was used to derive the frequency and amplitude modulations of the smoothed SW and FW oscillations. Frequency and amplitude modulations of SW and FW oscillations represent the temporal features of sleep EEG at different stages. Thus, the sleep stages can be automatically verified based on the features of sleep EEG.

In clinic, sleep EEG reflects the activities of cortices and HRV reflects the activity of ANS. The interaction between sleep EEG and HRV can be verified as the relationship between the temporal features of sleep EEG and DFA α_1 of HRV in comparison with the association between the power of delta band of sleep EEG and the normalized HF power of HRV in spectral analysis (Jurysta et al., 2003, 2006, 2010). The relationship between the features of EEG and DFA α_1 of HRV was verified by Pearson correlation coefficient with value of 0.512 ± 0.171. The association between the power of delta band of sleep EEG and the normalized HF power of HRV was also verified by Pearson correlation coefficient with value of 0.261 ± 0.212. Both results reflect a correlation between the activities of cortices and ANS. The relationship between the features of sleep EEG and DFA α_1 of HRV is more significant than the relationship verified by FFT-based methods.

2. Material and methods

2.1. Subjects

Gender differences can be observed in sleep parameters; to prevent confounding effects due to gender, we recruited only women for the present study. In total, 19 healthy women (aged 30.5 ± 3.4 years) were recruited. All subjects provided their informed consent, and the study was approved by the local IRB.

2.2. Polysomnography (PSG)

Standard overnight PSG was performed using a computerized sleep-scoring system under the continuous monitoring of board-certificated sleep technicians (Sandman; Tyco Ltd. Ottawa, Canada) in the sleep lab of the teaching hospital. The subjects in the PSG study were asked to maintain their usual sleep schedule for one week prior to the study. To minimize the interference of menstruation on sleep and pain, the PSG was conducted 7–10 days after each subject's last menstrual period. The PSG recordings began at the subjects' usual bedtime and ended at their usual waking time in the morning. The PSG recordings included 21 channels: 6 channels for EEG (C3/C4/O1/O2/A1/A2 in 10–20 systems), 2 channels for electrooculogram (EOG), 6 channels for electromyogram (EMG) over the submental and bilateral anterior tibialis muscle, 2 channels for electrocardiogram (ECG), 1 channel for a nasal cannula flow meter, 2 channels for abdomen and chest movement, 1 channel for pulse oximetry, and 1 channel for a position sensor. The temperature of the recording room was maintained between 24 and 26 °C. A blinded, board-certified, experienced sleep technician manually performed the PSG scoring in 30-second epochs following the R-K criteria (Rechtschaffen and Kales, 1968). The parameters for sleep onset latency, sleep efficiency, total sleep time, sleep stage, and other sleep events were scored accordingly. The raw data of the PSG were stored digitally for further processing and analysis. The sampling rate for the EEG and ECG was 128 Hz.

2.3. Decomposing sleep EEG into slow- and fast-wave oscillations by EMD

The EMD decomposes a time series into a set of intrinsic mode functions (IMFs) (Huang et al., 1998). An IMF must satisfy a necessary condition that the numbers of zero-crossings and extrema must be equal or at most differ by 1, and it guarantees a well-behaved Hilbert transform of the IMF. The relationships among the original signal, IMFs and the residue can be expressed as:

$$X(t) = \sum_{k=1}^{n} C_k(t) + R(t) \quad (1)$$

where $X(t)$ is the original time series; $C_k(t)$ is the kth IMF; n is the number of IMFs; and $R(t)$ is the residue.

The averaged period and energy density of an IMF can be determined by the following equations provided by Wu and Huang (2004) and the averaged frequency is the inverse of averaged period.

$$E_n = \frac{1}{N} \sum_{j=1}^{N} [C_n(j)]^2 \quad (2)$$

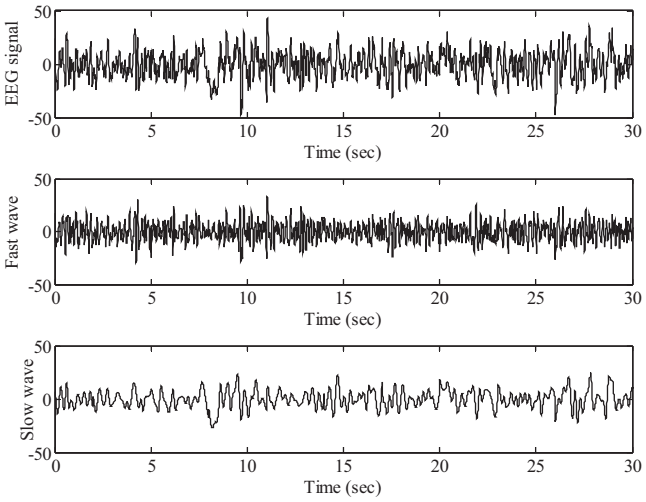

Fig. 1. An example of an EEG signal and its two major oscillations, slow- and fast-wave oscillations, decomposed by the enhanced EMD using masking signals.

$$\bar{T}_n = \int S_{\ln T,n} d\ln T \left(\int S_{\ln T,n} \frac{d\ln T}{T} \right)^{-1} \quad (3)$$

where E_n is the energy density of the nth IMF; $C_n(j)$ is the jth point of the nth IMF; $S_{\ln T,n}$ is the Fourier spectrum of the nth IMF as a function of $\ln T$, the period of the local wave form, and $\bar{T}_n$ is the averaged period of the nth IMF.

In this study, two major oscillations were used to depict the oscillatory fluctuations of sleep EEG: the slow-wave (SW) oscillation is the synthesis of the IMFs with averaged frequency less than 4 Hz; and fast-wave (FW) oscillation is the synthesis of the rest of IMFs. The mode mixing between two oscillations can be solved by adding masking signals (Deering and Kaiser, 2005). In this approach, the masking signal was added to the synthesis of two IMFs, with averaged frequencies around 4 Hz, for solving the mode-mixing between these two IMFs. The frequency of the masking signal was determined as the averaged frequency of the first IMF, which is decomposed from the synthesis by EMD. The amplitude of the masking signal was two times the averaged amplitude of the same IMF. Fig. 1 shows a sample of sleep EEG and its slow- and fast-wave oscillations.

2.4. Deriving amplitude and frequency modulations of slow- and fast-wave oscillations

Since both SW and FW oscillations are syntheses of multiple IMFs, the number of extrema is more than the number of zero-crossing. They do not satisfy the necessary condition for an IMF: the numbers of zero-crossings and extrema must be equal, or at most differed by one. Smoothing is a simple method, which can remove flutters and reserve the dominant oscillation of a signal. Therefore, the moving average with window sizes of 20 and 7 points was used to smooth the SW and FW oscillations. Then, the analytic representations of the smoothed oscillations can be derived by Hilbert transforms, and the time series of amplitude and phase can be derived from the analytic representations. Moreover, the time series of frequency can be derived as the first-order differential of phase time series. To assess the dominant frequency as a feature of sleep EEG, an amplitude-weighted frequency (AWF) for an instant is defined as:

$$F_{AW}(t) = \frac{A_s(t) \cdot F_s(t) + A_f(t) \cdot F_f(t)}{A_s(t) + A_f(t)} \quad (4)$$

where $F_{AW}(t)$ is amplitude-weighted frequency at instant t; $F_s(t)$ and $A_s(t)$ are instantaneous frequency and amplitude at instant t, respectively, for the SW oscillation; and $F_f(t)$ and $A_f(t)$ are the instantaneous frequency and amplitude at instant t, respectively, for the FW oscillation.

On the other hand, we also define the second factor as the mean amplitude of FW oscillation denoted as fast-wave mean amplitude (FWMA). To diminish the influence of spikes in the calculation of FWMA, it is defined as the geometric center of the amplitude histogram. A total of 120 bins, from 0 to 30 μV, were used to present the distribution of the FW oscillation for a short period. Amplitudes over 30 μV are counted as 30 μV in the histogram. The FWMA can be calculated by the following equation:

$$A_m = \frac{\sum_{a=1}^{120} A_a \cdot O_a}{\sum_{a=1}^{120} O_a} \quad (5)$$

where A_m is the mean amplitude; A_a is amplitude of the ath bin in the histogram; and O_a is the occurrence of samples with amplitude locals in the ath bin.

Undoubtedly, there are still many different parameters can be defined based on the frequency and amplitude modulations of SW and FW oscillations. AWF and FWMA are two of them, which represent significant correlations with sleep stages and ANS activity.

2.5. Monitoring ANS activity via DFA α1 of HRV

Detrended fluctuation analysis (DFA) is a tool for quantifying the fractal property of a time series (Peng et al., 1995a). In DFA, least-squares lines fit local data segments were used as the trends of data segments. Time scale, n, is defined as the length of data segments for fitting local trends. The fluctuation $F(n)$ is defined as the root-mean-square (RMS) energy of the detrended time series, in which the local trends with fitting time scale n has been removed. The power-law relationship between the time scales and their corresponding fluctuations represents the fractal property of the signal. In DFA, an integrating method can render an accumulated heartbeat time series as a fractal subject in profile (Peng et al., 1995b; Tulppo et al., 2005).

In many previous studies, a short-term scales from 4 to 11 beats and a long-term scales from 70 to 300 beats were used in human heartbeat time series analysis (Penzel et al., 2003; Kantelhardt et al., 2001). In these studies, the short-term scaling exponent denoted as DFA α_1 represents an assessment of the balance of vagal and sympathetic modulation. In this investigation, DFA α_1 was used to represent ANS activity during sleep. For monitoring ANS activity, the temporal values of DFA α_1 are calculated from the sliding windows of heartbeat time series with 32 successive beats, and the sliding window moves with a step length of four beats. A temporal value of DFA α_1 represents the ANS activity during a short time period.

3. Results

3.1. Characterize the temporal feature of sleep EEG in different sleep stages

To characterize the feature of sleep EEG using AWF and FWMA, the distributions of AWF and FWMA for different sleep stages were illustrated in Fig. 2. Each EEG segment with data length of 3 s was used for the calculations of AWF and FWMA. A total of 80 bins with frequency 0 to 16 Hz was used in the distribution of AWF, and 120 bins from 0 to 30 μV was used in the distribution of FWMA. AWF for NREM3 and NREM4 has a narrow distribution in low frequency band (<4 Hz). Thus, sleep EEG with AWF smaller than 4 Hz is defined as the "delta wave," referring to the definition of the delta wave

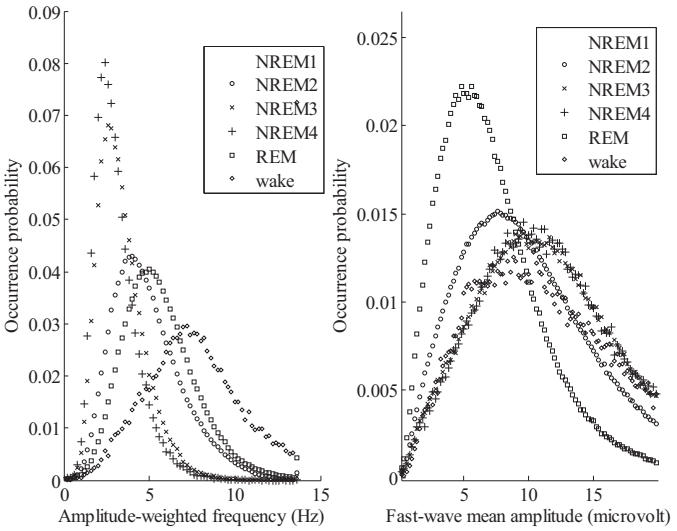

Fig. 2. Distributions of amplitude-weighted frequency (AWF) and mean amplitude of fast-wave oscillation (FWMA) for different sleep stages: (a) distributions for AWF; and (b) distributions for FWMA.

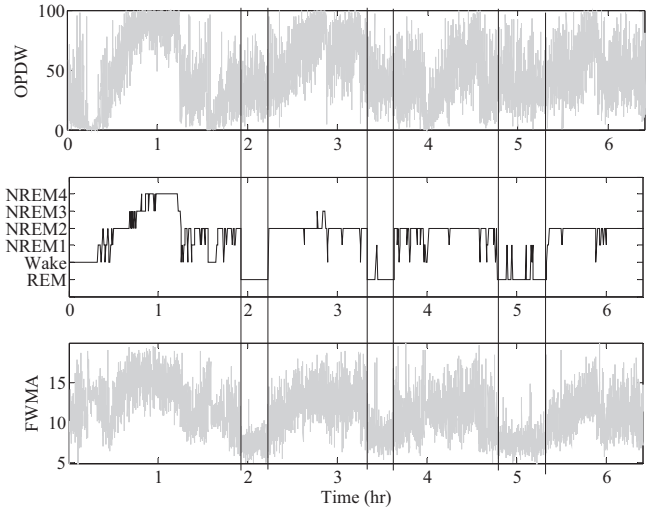

Fig. 3. Illustration of the continuous monitoring of sleep status using OPDW and FWMA compared with results verified by sleep technicians.

in traditional EEG spectral analysis. The occurrence probability for delta waves in an EEG segment with a short time period is a good index for assessing the sleep depth. Occurrence probability of delta wave is high in deep sleep stages (i.e., NREM3 and NREM4), and is low in light sleep stages (i.e., NREM1 and NREM2). The distribution of AWF for NREM1 is similar to that for REM sleep. On the other hand, FWMA for REM sleep has a narrow distribution with small value in the comparison with that for NREM1as shown in Fig. 2(b). The occurrence probability of delta wave (OPDW) was defined as an new index for a segment of sleep EEG. A time period of 3 s was used in the calculations of OPDW and FWMA to represent the temporal feature of sleep EEG. Both OPDW and FWMA vary with the sleep stages according to the distributions of AMF and FWMA.

During sleep, both OPDW and FWMA vary with the sleep stages. Fig. 3 shows a typical full course of sleep rated using OPDW and FWMA for comparisons with the sleep stages as normally verified by sleep technicians. As shown in Fig. 3, the OPDW correlates with the verified sleep stages, except for REM sleep. The OPDW during REM sleep is similar to that during NREM1. This result implies that REM and NREM1 have similar patterns in frequency modulation. OPDW does not act a good index for distinguishing NREM1 from REM. On the other hand, FWMA for REM sleep is lower than that for NREM1 as shown in the third subfigure of Fig. 3. Therefore, FWMA acts as a better parameter than OPDW does for distinguishing the temporal features of sleep EEG in REM and NREM1.

Statistical analysis of OPDW and FWMA for different sleep stages was derived from 19 sleep EEG recordings for healthy subjects. Fig. 4 shows the statistical results with box plots. Statistical difference between OPDW for REM and NREM1 is not significant. The values of OPDW are significantly different among different stages of NREM sleep as shown in Fig. 4(a). The statistical difference between the FWMA for NREM1 and REM is significant. The FWMA is correlatively low during REM sleep in comparison with that in NREM sleep. FWMA also significantly depends on the stages of NREM sleep as shown in Fig. 4(b).

3.2. Dynamics of HRV during sleep

Traditionally, spectral analysis of HRV presents sympathetic/parasympathetic tones in terms of the low-frequency power (LF), high-frequency power (HF), and the ratio of LF/HF, which

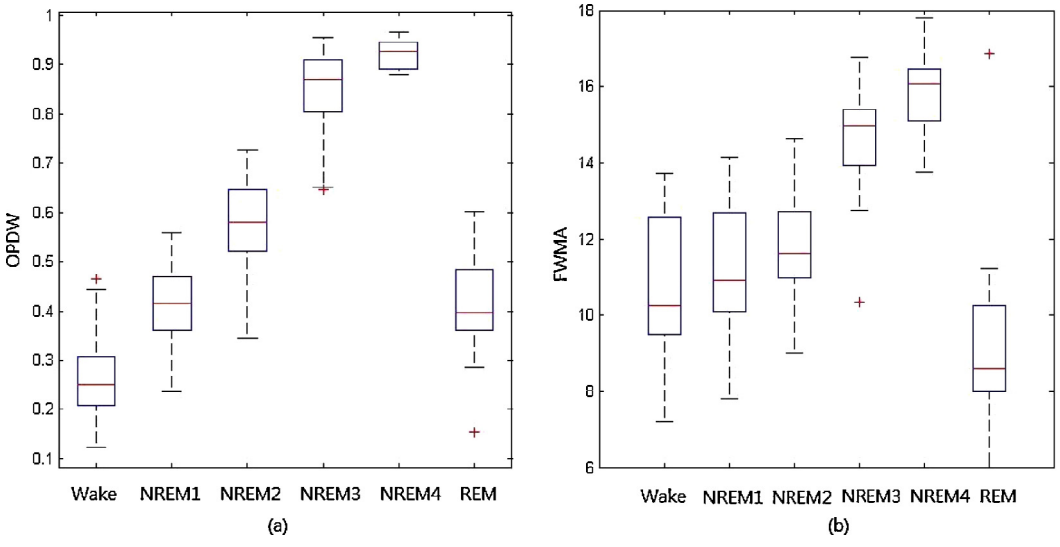

Fig. 4. Statistical results for OPDW and FWMA at different sleep stages.

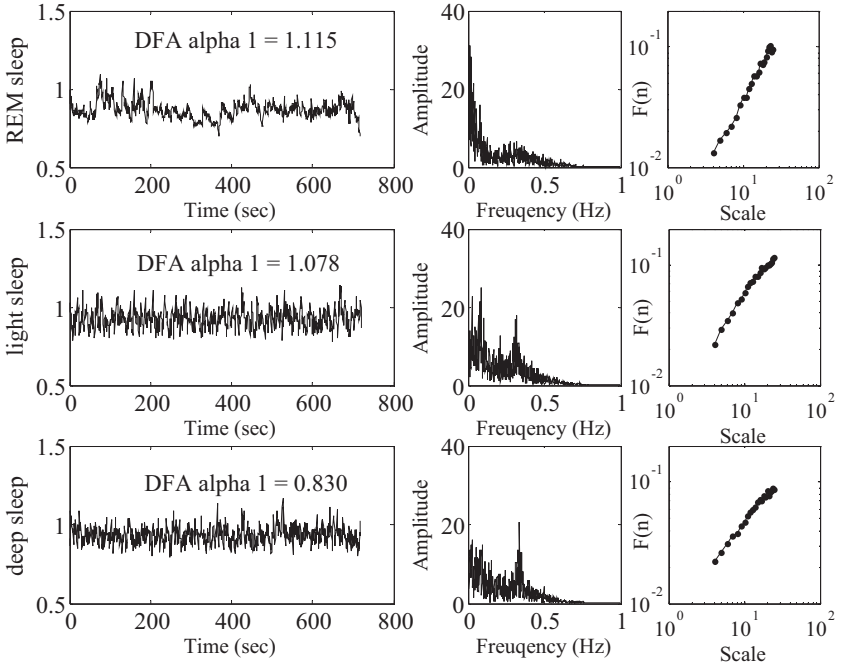

Fig. 5. Illustration of characteristics of the spectra and power-law correlations in DFA for light, deep and REM sleep stages.

correlate with stages. For a better understanding of the characteristics of HRV during sleep, spectral analysis and DFA were used to investigate the spectra and the short-term fractal property of HRV signals during different sleep stages. The HF of HRV is considered an indicator of parasympathetic and vagal tone. According to the HRV spectra shown in Fig. 5, the vagal tone of HRV during deep sleep (i.e., NREM3 and NREM4) is more significant than during light sleep (i.e., NREM1 and NREM2); it becomes insignificant during REM sleep. A previous literature (Penzel et al., 2003) reported that DFA α_1 reflects the balance of sympathetic and vagal modulations. The values of DFA α_1 significantly vary with sleep stages: 0.89 ± 0.19 for deep sleep (i.e., NREM3 and NREM4); 1.00 ± 0.21 for light sleep (i.e., NREM1 and NREM2); and 1.18 ± 0.24 for REM sleep. Referring the scale range defined in different references (Tulppo et al., 2001; Makikallio et al., 1997), a scale range from 4 to 11 was used for the calculations of DFA α_1 in this study. Fig. 6 shows the results of statistical analysis for 19 normal subjects. DFA α_1 for REM is significantly higher than those for NREM sleep, and DFA α_1 for light sleep is higher than for deep sleep.

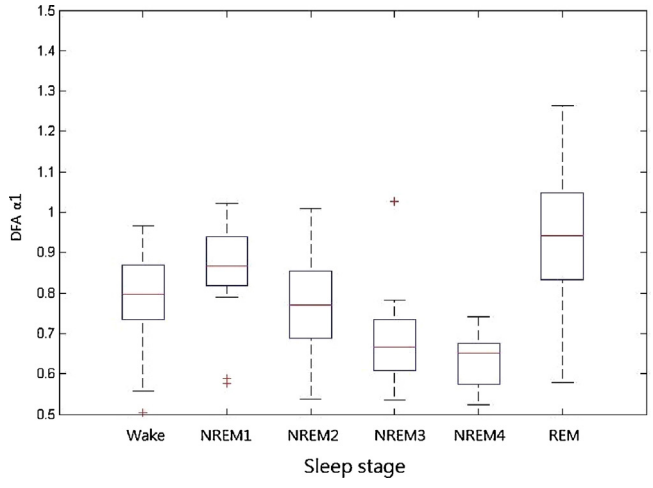

Fig. 6. Statistical results for DFA α_1 of HRV at different sleep stages.

3.3. Correlation between nonlinear modulations of sleep EEG and the sympathovagal tone of HRV

The dynamic interaction between sleep EEG and HRV has been investigated and reported in previous studies (Jurysta et al., 2003). Jurasta investigated the dynamic properties of sleep EEG and HRV, such as the delta-wave power and HF power of HRV. The reported interaction between sleep EEG and HRV was calculated using the Pearson correlation coefficient. The coefficient is approximately 0.4 between the delta power of EEG and the HF power of HRV, which represents a moderate correlation between the two factors. The dynamic interaction between sleep EEG and HRV analyzed using the FFT-based algorithm for one of the 19 subjects is shown in Fig. 7. The Pearson correlation coefficient between the delta power of EEG and HF power of HRV is 0.41. The dynamic interaction between FWMA of EEG and DFA α_1 of HRV for the same subject can be

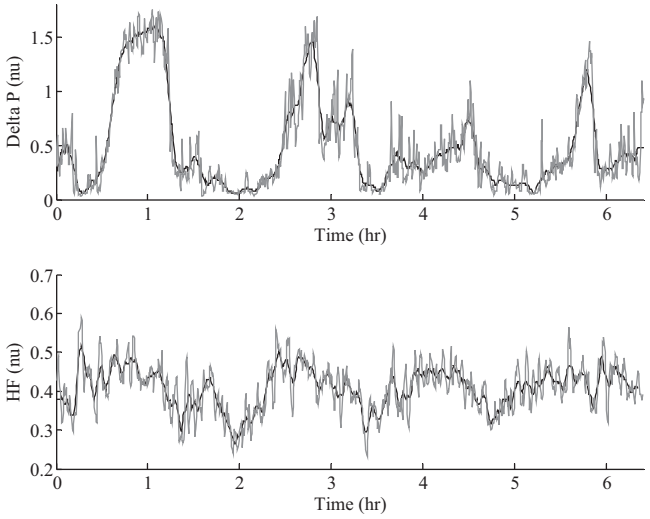

Fig. 7. Example of correlations between the delta power (Delta P) and normalized HF power of HRV for a normal subject.

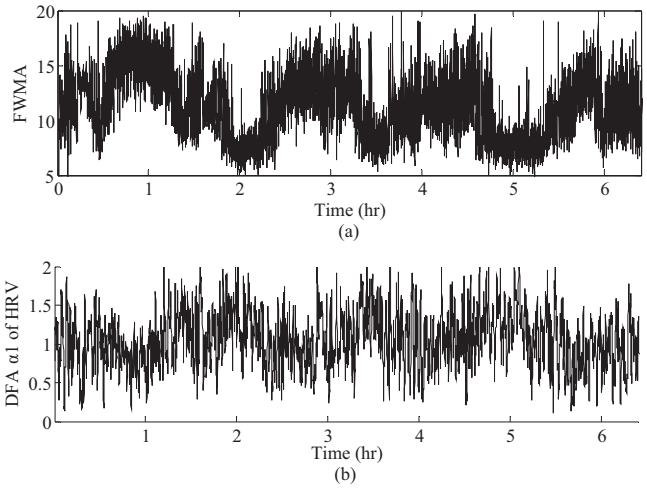

Fig. 8. Illustration of a negative correlation between the DFA α_1 of HRV and FWMA.

observed graphically, as shown in Fig. 8. A negative correlation between FWMA and DFA α_1 of HRV was affirmed with an absolute of 0.72. For the statistical results of 19 subjects, the interaction between sleep EEG and HRV represents an insignificant correlation of 0.261 ± 0.212 between the delta power of EEG and HF power of HRV by the FFT-based approach, and a significant correlation of 0.512 ± 0.171 between FWMA and DFA α_1 of HRV by the new approach based on HHT and DFA.

4. Discussion and conclusions

In this study, we introduce a new model for representing temporal features of sleep EEG. HHT acts to derive the frequency and amplitude modulations of slow- and fast-wave oscillations from sleep EEG. The parameter of AWF combines the instantaneous frequencies of slow- and fast-wave oscillations as a new property of sleep EEG at every instant. Delta wave is defined as an instant of EEG with AWF lower than 4 Hz. A time period of 3 s was used to calculate the OPDW. On the other hand, FWMA is a different parameter for representing the amplitude modulation of fast-wave oscillation. Both OPDW and FWMA serves as good indexes for verifying sleep stages.

OPDW is a good indicator for verifying different stages of NREM sleep, but according to our results, they do not effectively distinguish REM sleep, and thus, a different parameter was needed. The FWMA can distinguish REM sleep stages from NREM sleep stages, unlike the OPDW, which is similar to the delta power in a FFT-based analysis of EEG. Therefore, we propose the FWMA as an additional parameter with potential application in sleep medicine.

In addition, frequency modulation of fast-wave oscillation depicts a feature different from amplitude modulation of fast-wave oscillation. The instantaneous frequency of fast-wave oscillation during REM sleep is concentrated at the alpha band, and its mean amplitude is small. In contrast with the EEG of REM sleep, the instantaneous frequency of fast-wave oscillation scatters across a wide frequency band, from the theta band to the alpha band, and its mean amplitude is relatively large during NREM sleep. The details of frequency modulations in the fast-wave oscillation of sleep EEG, which are considered to imply complicated connections to different physiological mechanisms, are not discussed in this study.

Although the mechanism is not well-known, it has been demonstrated that higher general cardiac autonomic activity occurs in REM sleep and that comparatively decreased sympathetic tone and increased parasympathetic tone, along with increased sleep depth, occur in non-REM sleep. According to the results of previous studies, the dynamic interaction between sleep EEG and HRV can be quantified using the correlation coefficient between the delta power and HF power of HRV by an FFT-based approach; in this study, this FFT-based approach yields an insignificant correlation, with a Pearson correlation coefficient of approximately 0.261 ± 0.212 for all 19 subjects. This interaction is more significant (correlation coefficient 0.512 ± 0.171) when it is quantified by the correlation between the FWMA and DFA α_1 of HRV in the new approach based HHT and DFA.

The interactions between sleep EEG and HRV reflect significant variation among individuals in this study. Some subjects exhibit strong interactions between sleep EEG and HRV, with a correlation coefficient of 0.8, while for other subjects, the interaction is weak, with correlation coefficients of approximately 0.3. For subjects with strong interactions between sleep EEG and HRV, the DFA α_1 of HRV significantly depends on the sleep stages. However, the correlation between DFA α_1 of HRV and sleep stages is insignificant for subjects with weak interactions between sleep EEG and HRV. The DFA α_1 of HRV serves as an index of ANS activity during sleep, which is distinct from cortex activities reflected by sleep EEG.

In comparison with the delta power used as an indicator of sleep depth in NREM sleep, we found that the FWMA is more powerful for characterizing all sleep stages, including REM and NREM sleep. Furthermore, amplitude modulation appears as a relevant reverse-synchronizing behavior with DFA α_1 during sleep. Therefore, we hypothesize that this finding may imply an intrinsic structure and function for the underlying neuro-autonomic network during sleep.

In present study, we only focus on the analysis of delta oscillation and non-delta (fast-wave oscillation) of EEG because delta oscillation has been recognized to be associated with vagal activity during sleep and restorative function of normal sleep. Nevertheless, the other specific EEG frequency bands such as theta, gamma activity or sleep spindles play specific roles in REM sleep, memory consolidation, and sensory gating (Brankačk et al., 2012; Marshall et al., 2011; Montgomery et al., 2008; Cote et al., 2000). Based on our HHT based method, it is possible to characterize these specific oscillation modulations of sleep EEG. The interactions between these specific EEG modulations and other physiological status such as autonomic functions are worth to be further explored.

In conclusion, this study pioneers potential applications in sleep medicine. Nonlinearity and non-stationary characteristics are considered essentials of EEG and HRV. While traditional FFT has provided some interesting clinical applications, these methods should be improved with nonlinear signal processing and analysis algorithms. Here, we successfully applied two different nonlinear analysis algorithms of HHT and DFA to develop a new application for sleep medicine. These findings and technical improvements are the major contributions of this study.

Acknowledgements

The authors wish to express their gratitude for support from NSC (Taiwan, ROC), Grant No 99-2627-B-008-003, and 97-2314-B-038-002-MY3, joint foundation of NCU, Grant No CNJRF-99CGH-NCU-A3, VGHUST100- G1-4-3 and NSC support for the Center for Dynamical Biomarkers and Translational Medicine, National Central University, Taiwan (NSC 99-2911-I-008-100).

Appendix A. Supplementary data

Supplementary data associated with this article can be found, in the online version, at http://dx.doi.org/10.1016/j.jneumeth.2013.08.008.

References

Boettger S, Hoyer D, Falkenhahn K, Kaatz M, Yeragani VK, Bar KJ. Altered diurnal autonomic variation and reduced vagal information flow in acute schizophrenia. Clin Neurophysiol 2006;117:2715–22.

Brandenberger G, Ehrhart J, Piquard F, Simon C. Inverse coupling between ultradian oscillations in delta wave activity and heart rate variability during sleep. Clin Neurophysiol 2001;112:992–6.

Brankačk J, Scheffzük C, Kukushka VI, Vyssotski AL, Tort AB, Draguhn A. Distinct features of fast oscillations in phasic and tonic rapid eye movement sleep. J Sleep Res 2012;21:630–3.

Cote KA, Epps TM, Campbell KB. The role of the spindle in human information processing of high-intensity stimuli during sleep. J Sleep Res 2000;9:19–26.

Deering R, Kaiser JF. The use of a masking signal to improve empirical mode decomposition. Proc IEEE Int Conf Acoustics, Speech Signal Processing (ICASSP'05) 2005;4:485–8.

Ehrhart J, Toussaint M, Simon C, Gronfier C, Luthringer R, Brandenberger G. Alpha activity and cardiac correlates: Three types of relationships during nocturnal sleep. Clin Neurophysiol 2000;111:940–6.

Hall M, Vasko R, Buysse D, Ombao H, Chen Q, Cashmere JD, et al. Acute stress affects heart rate variability during sleep. Psychosom Med 2004;66:56–62.

Huang NE, Shen Z, Long SR, Wu MC, Shih HH, Zheng Q, et al. The empirical mode decomposition and the Hilbert spectrum for nonlinear and non-stationary time series analysis. Proc R Soc Lond A 1998;454:903–95.

Jurysta F, Borne P, Migeotte PF, Dumont M, Lanquart JP, Degaute JP, et al. A study of the dynamic interactions between sleep EEG and heart rate variability in healthy young men. Clin Neurophysiol 2003;114:2146–55.

Jurysta F, Lanquart JP, Borne P, Migeotte PF, Dumont M, Degaute JP, et al. The link between cardiac autonomic activity and sleep delta power is altered in men with sleep apnea-hypopnea syndrome. Am J Physiol Regul Integr Comp Physiol 2006;291:R1165–71.

Jurysta F, Kempenaers C, Lancini J, Lanquart JP, Borne P, Linkowski P. Altered interaction between cardiac vagal influence and delta sleep EEG suggests an altered neuroplasticity in patients suffering from major depressive disorder. Acta Psychiatr Scand 2010;121:236–9.

Kantelhardt JW, Koscielny-Bunde E, Rego HHA, Havlin S, Bunde A. Detecting long-range correlations with detrended fluctuation analysis. Physica A 2001;295:441–54.

Makikallio TH, Seppänen T, Airaksinen KEJ, Koistinen J, Tulppo MP, Peng CK, et al. Dynamic analysis of heart rate may predict subsequent ventricular tachycardia after myocardial infarction. Am J Cardiol 1997;80:779–83.

Marshall L, Kirov R, Brade J, Mölle M, Born J. Transcranial electrical currents to probe EEG brain rhythms and memory consolidation during sleep in humans. PLoS ONE 2011;6:e16905.

Mina A, Tokuhiro K, Sunao U, Shinchi M, Kyoko N, Junko M, et al. Correlation between electroencephalography and heart rate variability during sleep. Psychiatry Clin Neurosci 2003;57:59–65.

Montgomery SM, Sirota A, Buzsáki G. Theta and gamma coordination of hippocampal networks during waking and rapid eye movement sleep. J Neurosci 2008;28:6731–41.

Otzenberger H, Simon C, Gronfier C, Brandenberger G. Temporal relationship between dynamic heart rate variability and electroencephalographic activity during sleep in man. Neurosci Lett 1997;229:173–6.

Otzenberger H, Gronfier C, Simon C. Dynamic heart rate variability: a tool for exploring sympathovagal balance continuously during sleep in men. Am J Physiol 1998;275:H946–50.

Peng CK, Havlin S, Hausdorff JM, Mietus JE, Stanley HE, Goldberger AL. Fractal mechanisms and heart rate dynamics. Long-range correlations and their breakdown with disease. J Electrocardiol 1995a;28:59–65.

Peng CK, Havlin S, Stanley HE, Goldberger AL. Quantification of scaling exponents and crossover phenomena in nonstationary heartbeat time series. Chaos 1995b;5:82–7.

Penzel T, Kantelhardt JW, Grote L, Peter JH, Bunde A. Comparison of detrended fluctuation analysis and spectral analysis for heart rate variability in sleep and sleep apnea. IEEE Trans Biomed Eng 2003;50:1143–51.

Rechtschaffen A, Kales A. A manual standardized terminology, techniques and scoring system for sleep stages of human subjects. Public Health Service. NIH Publication No. 204. Washington, DC: US Government Printing Office; 1968.

Roche F, Gaspoz JM, Fortune IC, Minini P, Pichot V, Duverney D, et al. Screening of obstructive sleep apnea syndrome by heart rate variability analysis. Circulation 1999;100:1411–5.

Tasali E, Leproult R, Ehrmann DA, Cauter EV. Slow-wave sleep and the risk of type 2 diabetes in humans. Proc Natl Acad Sci U S A 2008;105:1044–9.

Tulppo MP, Hughson L, Kikallio THM, Airaksinen KEJ, Nen TS, Huikuri KV. Effects of exercise and passive head-up tilt on fractal and complexity properties of heart rate dynamics. Am J Physiol Heart Circ Physiol 2001;280:H1081–7.

Tulppo MP, Kiviniemi AM, Hautala AJ. Physiological background of the loss of fractal heart rate dynamics. Circulation 2005;112:314–9.

Uchida S, Maloney T, Feinberg I. Beta (20–28 Hz) and delta (0.3–3 Hz) EEGs oscillate reciprocally across NREM and REM sleep. Sleep 1992;15:352–8.

Uchida S, Maloney T, Feinberg I. Sigma (12–16 Hz) and beta (20–28 Hz) EEG discriminate NREM and REM sleep. Brain Res 1994;659:243–8.

Uchida S, Feinberg I, March JD, Atsumi Y, Maloney T. A comparison of period amplitude analysis and FFT power spectral analysis of all-night human sleep EEG. Physiol Behav 1999;67:121–31.

Wu Z, Huang NE. A study of the characteristics of white noise using the empirical mode decomposition method. Proc R Soc Lond A 2004;460:1597–611.